Electronic Supplementary Material (ESI) for RSC Advances.
This journal is © The Royal Society of Chemistry 2016

Electronic Supporting Information (ESI)

Functional organogelators formed by liquid-crystal carbazole-containing *bis*-MPA dendrimers

I. Gracia,[a] J. L. Serrano,[b] J. Barberá[a] and A. Omenat*[a]

General methods and materials

Starting chemicals and solvents were purchased from commercial sources and used without further purification, excepting carbazole that was recrystallized from ethanol and dicloromethane. The structural characterisation of compounds was done by ^{1}H NMR, ^{13}C NMR, IR spectroscopy, mass spectrometry and elemental analysis. NMR experiments were performed on a Bruker AVANCE 400 and a Bruker ARX 300 spectrometers. Infrared spectra of the compounds and gels were recorded on a Bruker Tensor27 spectrophotometer on KBr pellets for solids and NaCl windows for gels. Mass spectrometry analysis was performed in a Bruker Microflex spectrometer. Elemental analysis were measured in a Perkin Elmer 2400 microanalyser. UV-vis and fluorescence spectra were collected from an ATI-Unicam UV4-200 and Perkin-Elmer LS50B spectrophotometers respectively, using quartz cuvettes. Cyclic voltammetry was performed in an AUTOLAB PGSTAT204 instrument using a three electrode cell, with ITO working electrode, platinum wire as counter-electrode and Ag/AgCl as reference electrode. FE-SEM microscopy was performed in a Carl Zeiss Merlin microscope operating at low voltages and TEM on a FEI TECNAI T20 microscope operating at 20 KeV.

Mesogenic behaviour and transition temperatures were determined using an Olympus BH-2 polarizing microscope equipped with a Linkam TMS91 hot-stage and a CS196 hot-stage central processor. DSC TA Instruments Q-20 and Q-2000 systems were used to carry out differential scanning calorimetry experiments. Samples were sealed in aluminum pans and a scanning rate of 10 ºC minute^{-1} under a nitrogen atmosphere was used. Temperatures are taken from the onset of the peak unless otherwise noted. Thermogravimetric analyses (TGA) were performed using a TA Instrument TGA Q5000 at a rate of 10 ºC/minute under a nitrogen atmosphere. X-ray diffraction experiments of the mesophases were performed in a pinhole camera (Anton-Paar) operating with a point focused Ni-filtered Cu-Kα beam. Lindemann glass capillaries with 0.9 mm inner diameter were used to contain the sample. The capillary axis was held vertical and the pattern collected on flat photographic film. Bragg´s law was used to calculate the *d* spacings.

Experimental

Synthesis

The synthesis of **1**, **2**, **3** and **4** was already described elsewhere[42].

General procedure for the synthesis of **5** and **6**. Example for **5**.

To a solution at 0 ºC of 5(N-carbazoyl)-N-(2-hydroxyethyl)pentanamide (34 mg, 0.11 mmol), the mesogenic dendron **2** (200 mg, 0.10 mmol) and DPTS (6 mg, 0.02 mmol) in dry CH_2Cl_2, was added a solution of DCC (25 mg, 0.12 mmol) in dry CH_2Cl_2 dropwise. The reaction was stirred overnight at room temperature. The insoluble DCU byproduct was filtered off through a Celite® pad and the crude product was purified by recrystallisation in EtOH. A white solid is obtained.

5

Yield 99 mg (43 %). **^{1}H NMR** (400 MHz, CD_2Cl_2) δ (ppm): 8.15 – 8.06 (m, 10H, ArH), 8.06 – 8.01 (m, 8H, ArH), 7.45 – 7.38 (m, 4H, ArH), 7.31 – 7.23 (m, 8H, ArH), 7.18 (ddd, *J* = 8.0, 5.1, 3.0 Hz, 2H, ArH), 7.02 – 6.92 (m, 8H, ArH), 6.08 (t, *J* = 5.7 Hz, 1H, NH), 4.60 – 4.46 (m, 10H, OCH_2 + NCH_2), 4.40 – 4.24 (m, 4H, OCH_2), 4.11 – 4.01 (m, 8H, OCH_2), 3.99 (t, *J* = 5.5 Hz, 2H, OCH_2), 3.40 – 3.32 (m, 2H, NCH_2), 2.15 (t, *J* = 7.4 Hz, 2H, $alCH_2$), 1.91 – 1.74 (m, 10H, $alCH_2$), 1.76 – 1.63 (m, 2H, $alCH_2$), 1.54 – 1.39 (m, 8H, $alCH_2$), 1.47 (s, 3H, CH_3), 1.39 (s, 6H, CH_3), 1.37 – 1.24 (m, 64H, $alCH_2$), 0.96 – 0.85 (m, 12H, CH_3). **^{13}C NMR** (100 MHz, CD_2Cl_2) δ (ppm): 173.26, 173.01, 172.75, 172.65, 165.79, 165.75, 165.71, 165.70, 164.82, 164.75, 164.42, 155.72, 140.95, 132.82, 131.68, 127.59, 126.19, 123.26, 122.62, 121.57, 120.74, 119.29, 114.93, 109.33, 69.06, 66.69, 54.54, 54.27, 54.00, 53.73, 53.46, 49.96, 47.50, 47.46, 47.24, 43.37, 38.76, 36.39, 32.52, 30.27, 30.26, 30.23, 30.19, 30.16, 29.96, 29.94, 29.69, 29.11, 26.54, 23.86, 23.28, 18.47, 17.96, 14.47. **IR** $\tilde{\nu}$ (KBr, cm^{-1}): 3407 (N-H), 3078, 2926 (Csp^3-H), 2855 (Csp^3-H), 1734 (ancha, C=O), 1650, 1605. **MS** (MALDI-TOF) m/z: 2315.5 $[M+Na]^+$. **Elemental analysis**: calculated for $C_{138}H_{174}N_2O_{27}$: C, 72.79; H, 7.65; N, 1.32. Found: C, 73.03; H, 7.48; N, 1.42.

6

Yield 67 mg **(**42 %). **^{1}H NMR** (400 MHz, CD_2Cl_2) δ (ppm): 8.17 – 7.97 (m, 18H, ArH), 7.46 – 7.35 (m, 4H, ArH), 7.33 – 7.21 (m, 8H, ArH), 7.18 (ddd, *J* = 7.9, 6.4, 1.7 Hz, 2H, ArH), 7.05 – 6.90 (m, 8H, ArH), 6.34 (t, *J* = 5.6 Hz, 1H, NH), 4.65 – 4.44 (m, 12H, OCH_2 + NCH_2), 4.40 – 4.22 (m, 8H, OCH_2), 4.08 – 3.98 (m, 8H, OCH_2), 3.96 (t, *J* = 5.5 Hz, 2H, OCH_2), 3.30 (q, *J* = 5.4 Hz, 2H, NCH_2),

2.27 (t, *J* = 7.4 Hz, 4H, $OCCH_2$), 1.89 – 1.74 (m, 12H, $alCH_2$), 1.66 – 1.57 (m, 8H, $alCH_2$), 1.52 – 1.43 (m, 16H, $alCH_2$), 1.43 – 1.22 (m, 60H, $alCH_2$), 1.21 (s, 3H, CH_3), 1.19 (s, 6H, CH_3), 1.18 (s, 3H, CH_3), 0.97 – 0.84 (m, 12H, CH_3). **^{13}C NMR** (100 MHz, CD_2Cl_2) δ (ppm): 173.25, 173.03, 172.96, 172.79, 172.68, 165.77, 165.73, 165.68, 164.79, 164.74, 164.41, 164.40, 155.71, 140.93, 132.80, 131.68, 127.68, 127.60, 126.20, 123.27, 122.62, 122.57, 121.63, 121.57, 120.76, 119.34, 114.92, 109.27, 69.05, 66.64, 66.49, 47.48, 47.45, 47.25, 46.53, 43.20, 34.18, 32.51, 30.25, 30.23, 30.19, 30.16, 29.95, 29.94, 29.69, 28.95, 26.54, 23.28, 23.13, 18.45, 18.12, 17.95, 14.46. **IR** $\tilde{\nu}$ (KBr, cm^{-1}): 3426 (N-H), 3075, 2926 (Csp^3-H), 2855 (Csp^3-H), 1734 (C=O), 1650, 1605. **MS** (MALDI-TOF) m/z: 2681.4 $[M+Na]^+$. **Elemental analysis**: calculated for $C_{160}H_{197}N_3O_{31}$: C, 72.79; H, 7.47; N, 1.58. Found: C, 72.91; H, 7.32; N, 1.71.

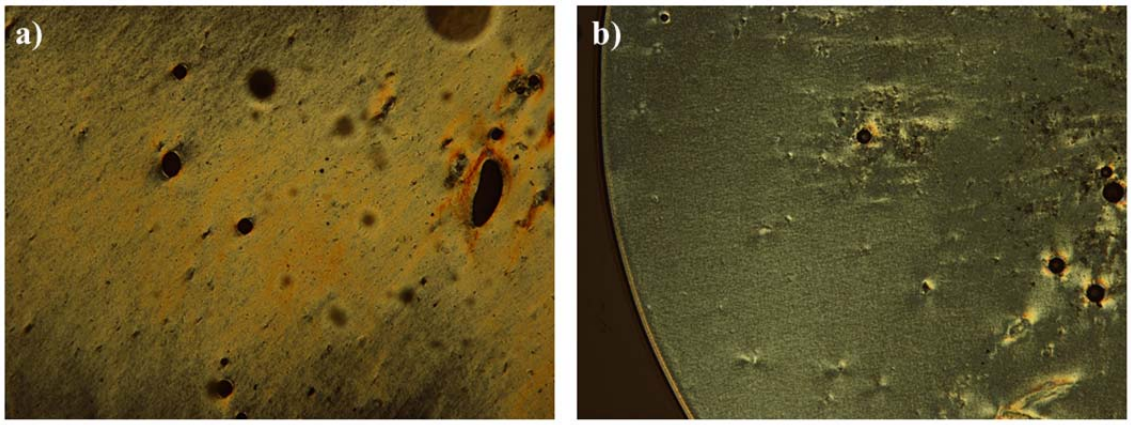

Fig. S 1. POM microphotographs of the SmC mesophase of compound **5** at 60 ºC (a) and compound **6** at 50 ºC (b).

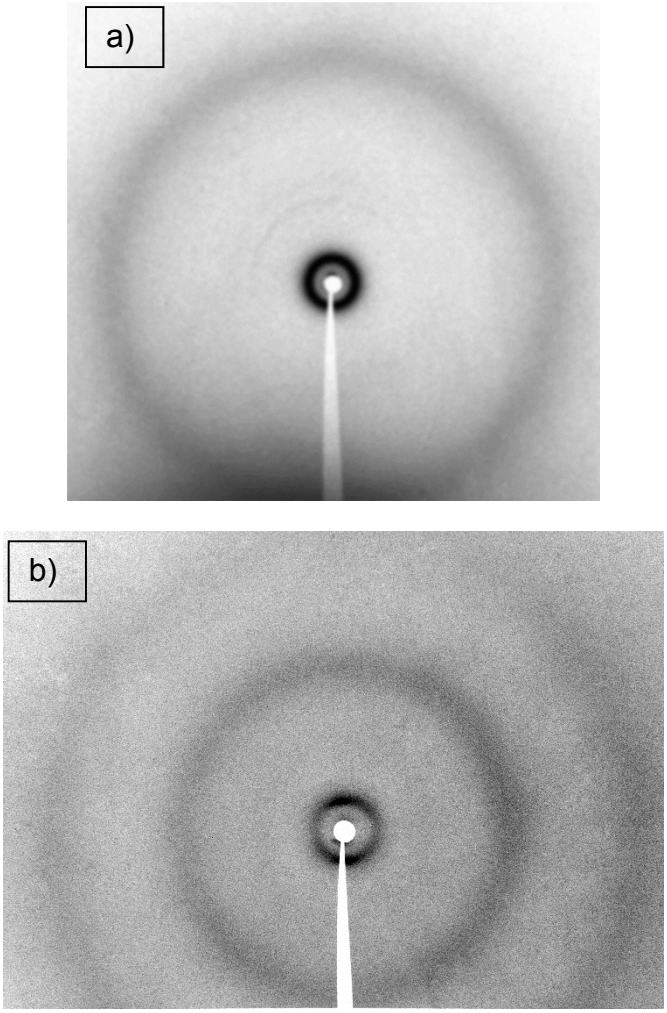

Fig. S 2. X-ray diffractograms of compounds: a) **3** at room temperature after cooling from the isotropic state. b) **4** at room temperature after cooling from the isotropic state. Partially oriented sample.

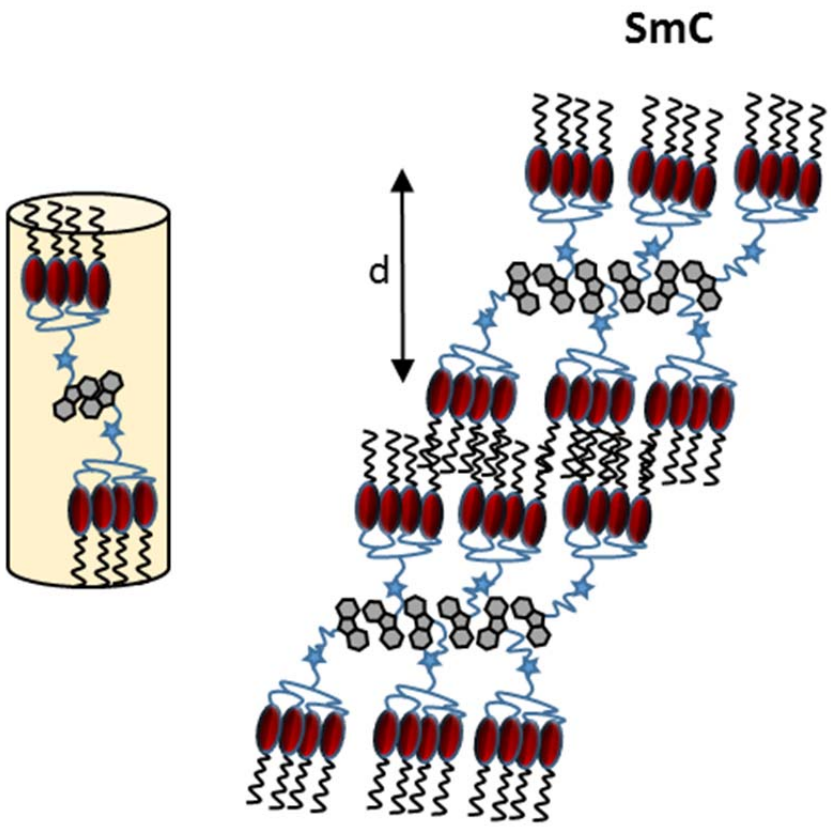

Fig. S 3. Schematic model proposed for the supramolecular organisation in the SmC mesophase of compound **5**.

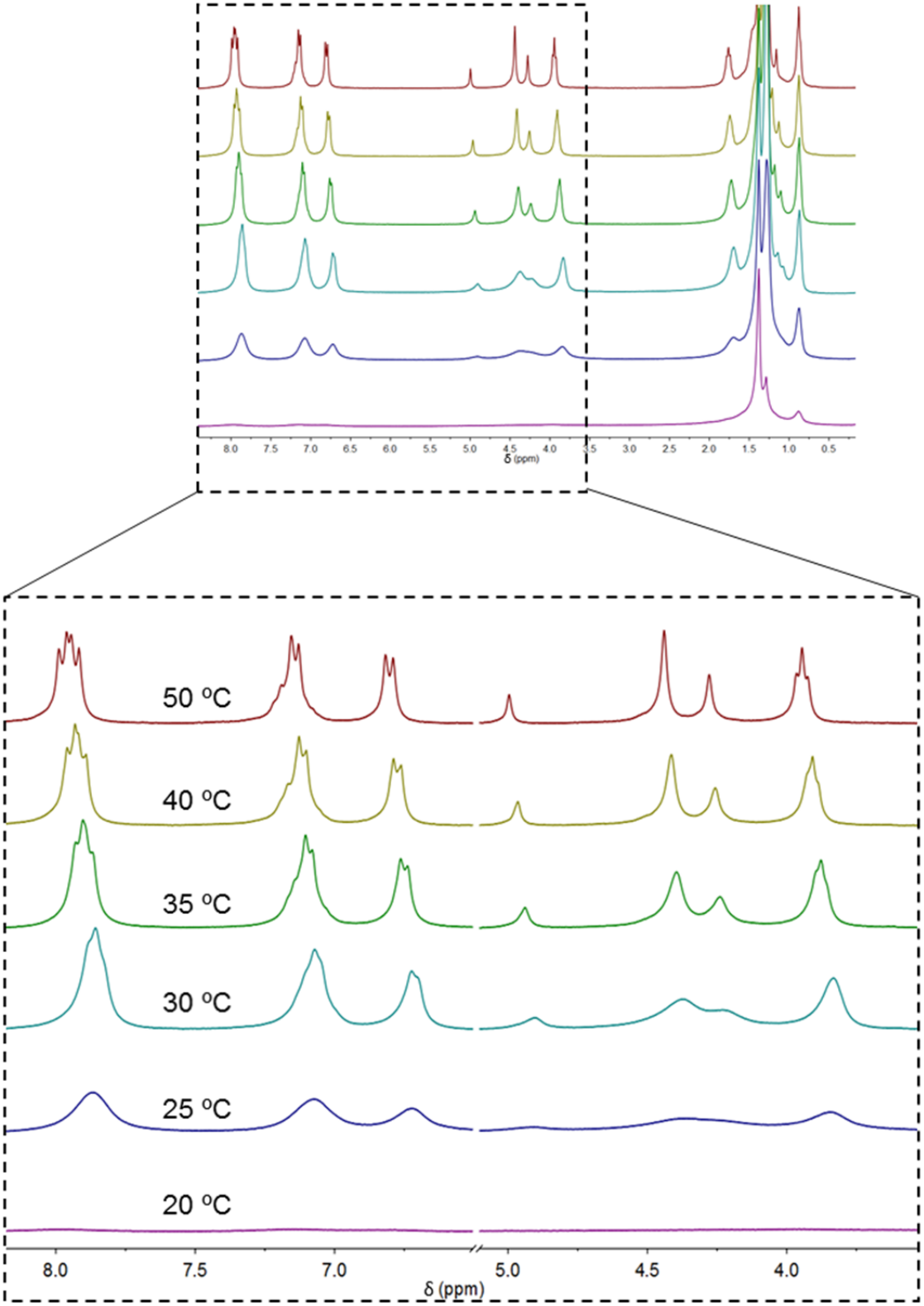

Fig. S 4. Variable temperature ^{1}H NMR spectra of compound **1** at 2.5 %wt. in cyclohexane-d_{12}. Cooling from the sol to the gel.

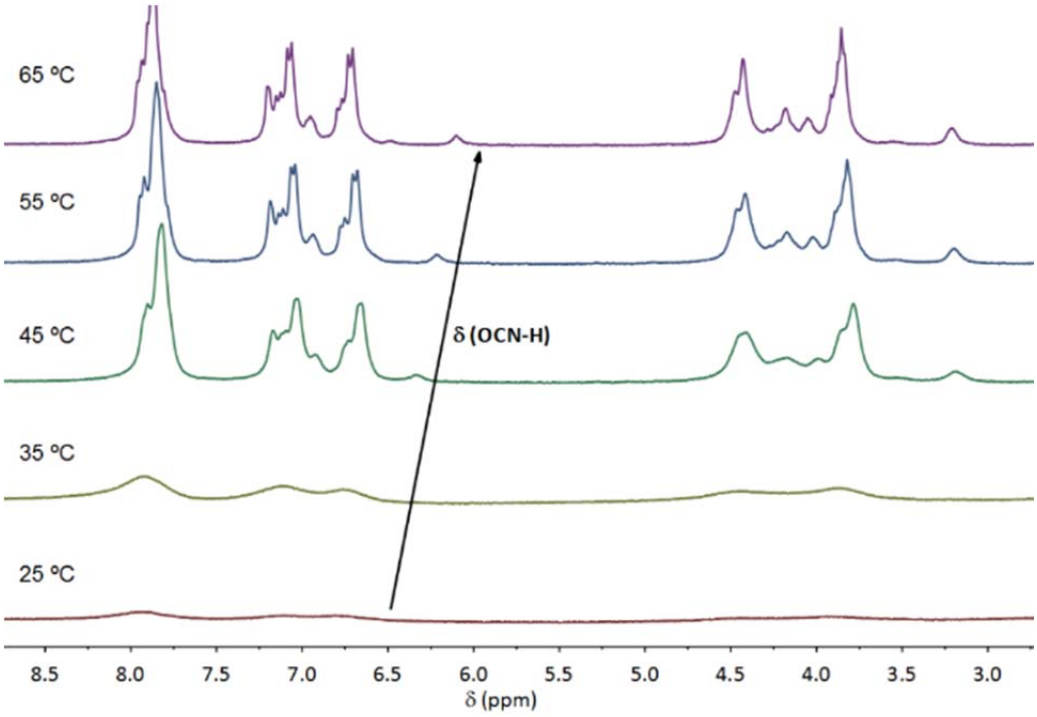

Fig. S 5. ^{1}H NMR spectra of **5** at 2 %wt. in cyclohexane-d_{12} at increasing temperatures.

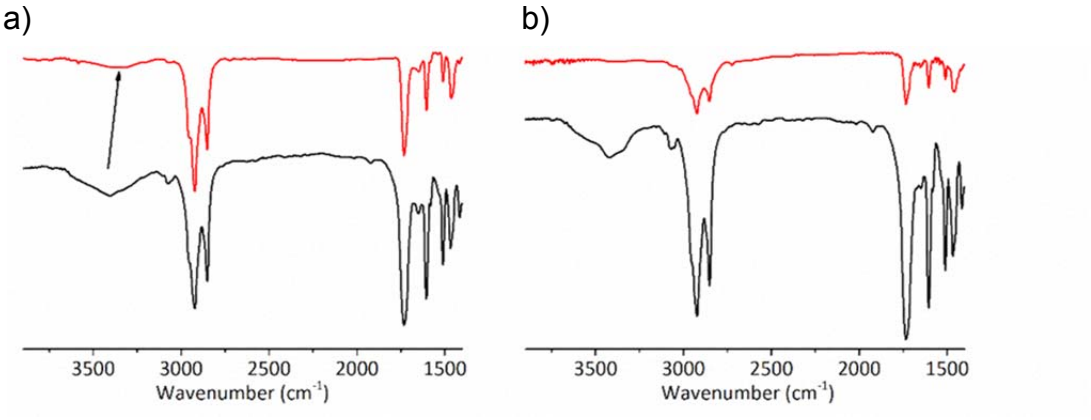

Fig. S 6. IR spectra of compounds: a) **5** and b) **6,** in the gel (red) and solid (black) state.

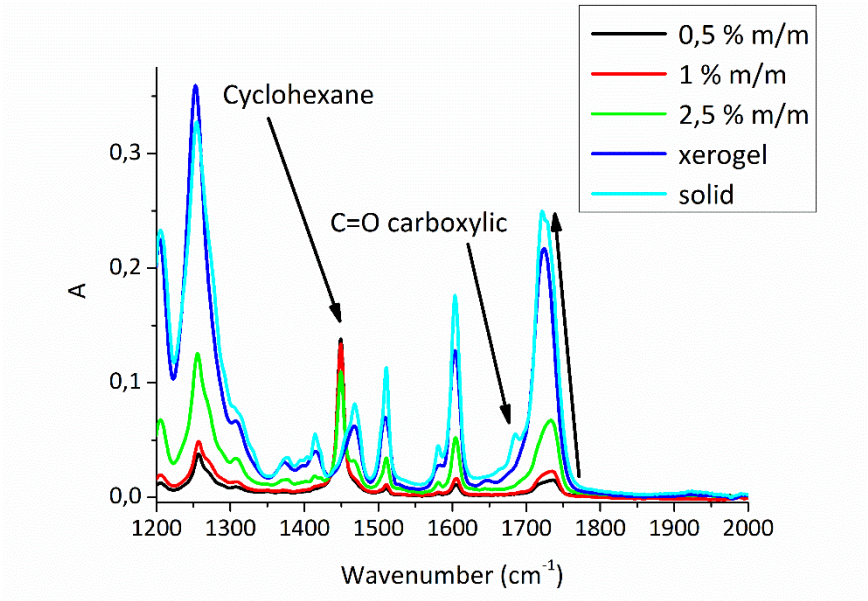

Fig. S 7. Concentration dependent IR spectra of xerogels of **2** in cyclohexane.

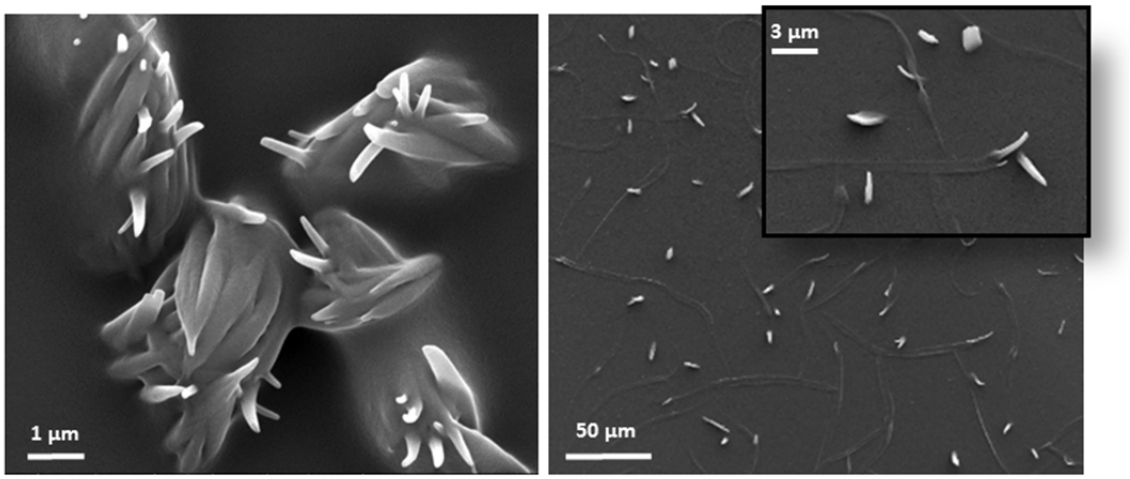

Fig. S 8. FE-SEM images from xerogels in cyclohexane: a) Compound **2** (1 %wt.), b) Compound **5** (1 %wt.).

a)

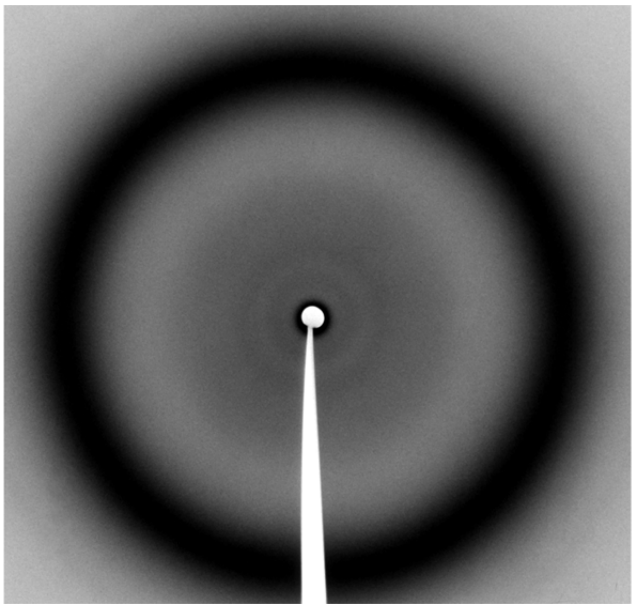

b)

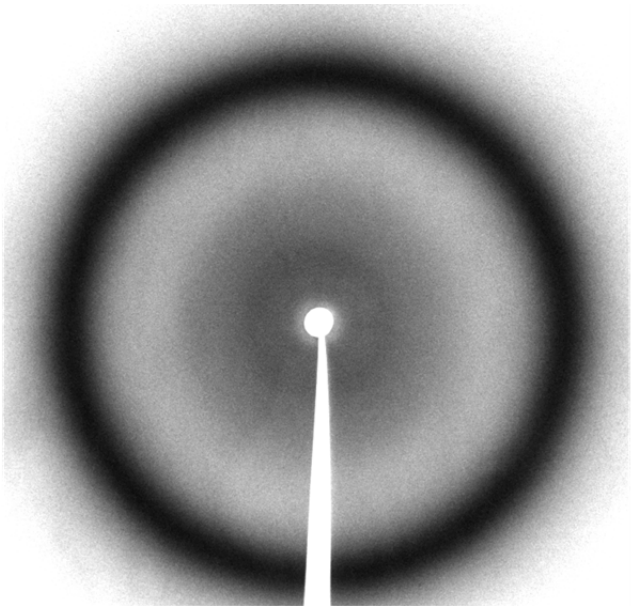

Fig. S 9. XRD diffractograms of the xerogels. a) Compound **2**; b) Compound **3**.

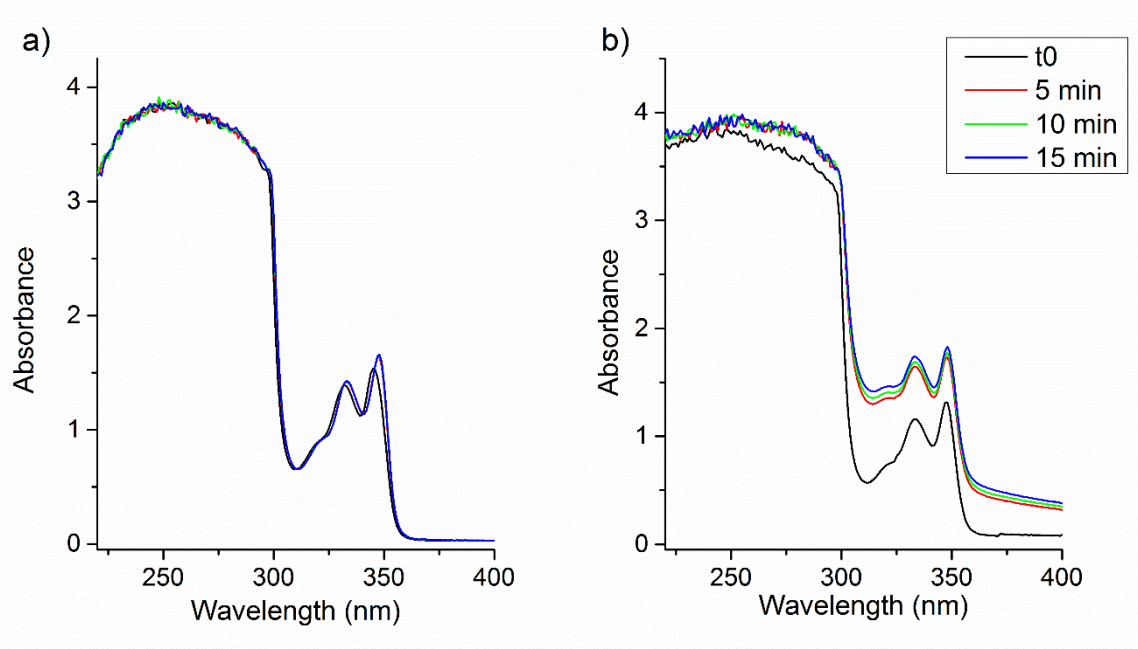

Fig. S 10. UV-vis spectra of the organogels **5** and **6** in cyclohexane (0.5 %wt.).

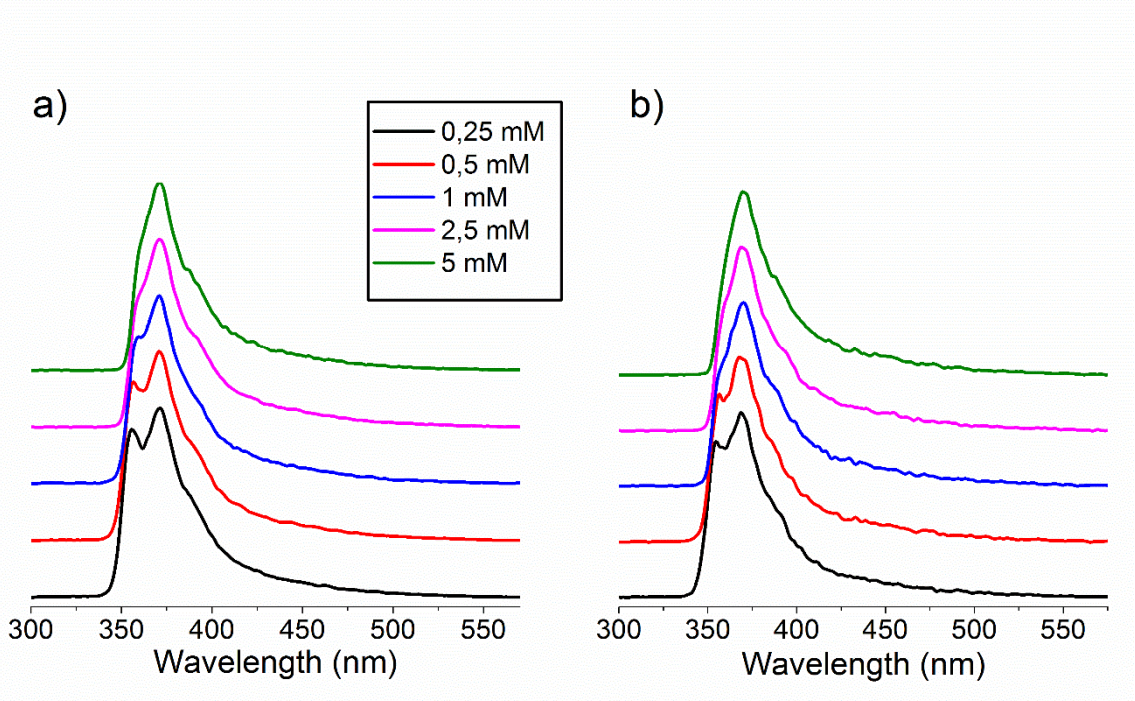

Fig. S 11. Fluorescence emission spectra of compound **5** (a) and compound **6** (b) in cyclohexane at different concentrations.

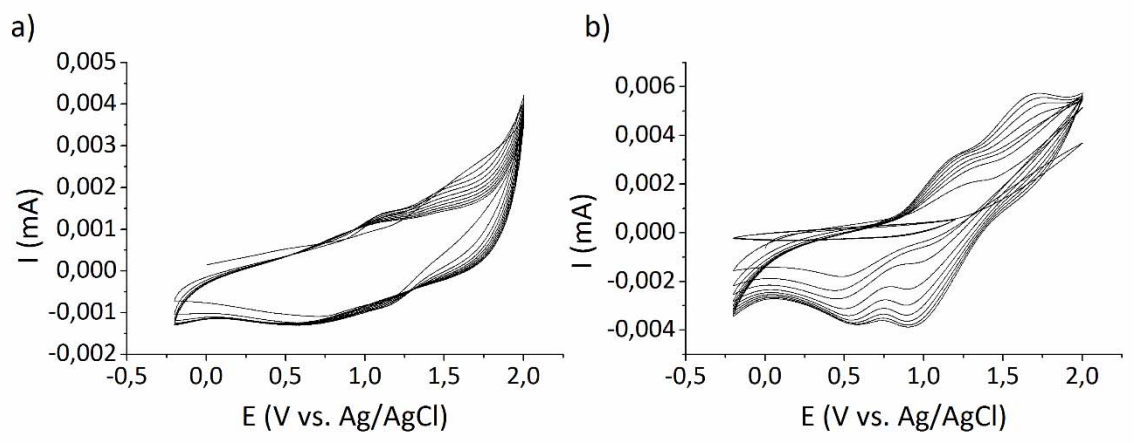

Fig. S 12. CV traces of the modified ITO-electrodes with compounds of 5 (a) and 6 (b) xerogels from cyclohexane (100 mV s^{-1}, o.1 M $(n\text{-}Bu)_4N(PF_6)$ in acetonitrile).